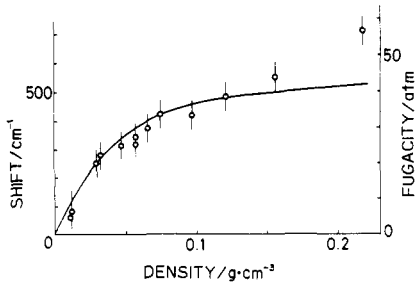

Figure 6. Comparison between the observed solvatochromic shifts (O) and the reported fugacities (—) as a function of ethane density.

molecule, the best fit was obtained between experimental solvatochromic shifts and those estimated from eq 12. The results are given in Figure 6. The agreement is excellent especially in the low-density region. This indicates that the argument given in section C is reasonable, and the cluster size distribution in the low-density region can well be represented by the Poisson distribution. The shift predicted for each ethane molecule, 180 cm^{-1}, is smaller than that of DMABN–CF_3H system ($\Delta\nu$ = 225 cm^{-1}).[6] This trend is of course consistent with the tendency in mutual virial coefficients B_{12}, which reflects the strength of intermolecular interaction; B_{12} = −750 cm^{-1} for DMABN–C_2H_6 and −1400 cm^{-1} for the DMABN–CF_3H system.[6]

(F) Cluster Size Distribution and the Molecular Interaction. It is experimentally apparent that the bathochromic shift shows a leveling off as the density of the solvent fluid increases. This means that the number of solvating molecules is not linearly dependent on the density of bulk fluid. Such a saturation behavior can be mainly attributed to the following two reasons. The first cause is the intermolecular interaction among solvent molecules not adsorbed on DMABN, i.e., an external effect. In other words, mutual attraction within solvent molecules suppresses the transferability of an individual molecule from bulk solvent phase to the cluster. As the density of the bulk phase increases, such an effect is enhanced owing to the increasing intermolecular attraction, and hence the transferability becomes saturated. Experimentally, "fugacity" or chemical potential of the solvent expresses this transferability. This is the reason the observed bathochromic shift is proportional to the fugacity of bulk solvent especially in the low-density region.

The second cause is the saturation of the clustering molecules in the first solvation shell around the polar solute. That is, the intermolecular interaction among adsorbed solvent molecules, i.e., internal effect, prevents an additional solvent molecule from entering into the solvation shell. This effect must be dominant especially in the high-density region. The simplest way of including such an effect may be the assumption of a Langmuir type equilibrium adopted in the previous paper. To consider this effect in a more sophisticated manner, an accurate calculation to estimate the partition function of a cluster will be needed.

In the present investigation, the solvatochromic shift is mainly analyzed under the assumption that the first cause is dominant. In other words, the adsorbed solvent molecules are assumed to be independent with each other. This means that the present discussion is applicable mainly to a supercritical fluid solution of low density or to small size clusters.

Conclusions

The solubility and the solvatochromic shift of 4-(dimethylamino)benzonitrile (DMABN) in supercritical ethane was measured in varying densities. From the density dependence of the solubility, the mutual virial coefficient B_{12} was estimated to be −750 cm^3/mol. From the relation between B_{12} and the intermolecular potential, the potential function $V(r,\vartheta)$ between DMABN and ethane was deduced.

The solvatochromic shift was found to be much larger than expected from Onsager's theory. This indicates that solvent molecules aggregate around solute molecules and form clusters even in a nonpolar supercritical fluid like ethane. Therefore, we explained the solvatochromic shift not from Onsager's model, which regards solvent as uniform continuum, but from a picture that clusters of various size are distributed in supercritical fluid.

To estimate the cluster size distribution in supercritical solution of given density, we adopted a statistical mechanical approach using a grand canonical ensemble. The size distribution was found to be given by a Poisson distribution, and the average number of solvating molecules was expressed as a function of solvent–solute interaction and fugacity of the solvent of a given density. The average solvation number thus obtained was found to be in good agreement with the observed solvatochromic shift. From the proportionality constant in the above relation, we determined the bathochromic shift per each solvating ethane molecule to be 180 cm^{-1}.

Acknowledgment. This work was supported by a Grant-in-aid (No. 01606001) from the Ministry of Education, Japan.

Registry No. DMABN, 1197-19-9; C_2H_6, 74-84-0.

Isolated Redox Centers within Microporous Environments. 1. Cobalt-Containing Aluminophosphate Molecular Sieve Five

Consuelo Montes,[†] Mark E. Davis,*[,†] Brendan Murray,[‡] and Mysore Narayana[‡]

Department of Chemical Engineering, Virginia Polytechnic Institute and State University, Blacksburg, Virginia 24061, and Shell Development Company, Westhollow Research Center, Houston, Texas 77001

(Received: October 2, 1989; In Final Form: March 27, 1990)

Cobalt-containing aluminophosphate five (CoAPO-5) was synthesized and shown to contain tetrahedral Co^{2+} residing within framework atomic positions and also as extraframework cations. The isolated framework Co^{2+} atoms can be oxidized by O_2 at 500 °C to Co^{3+} which is stabilized in tetrahedral coordination by the oxide lattice. The framework Co^{3+} is easily reduced to Co^{2+} by a variety of reducing agents.

Introduction

Zeolites and other molecular sieves are well known for their ability to function as shape-selective, solid acid catalysts.[1] Deposition of metals into the microporous voids of zeolites has yielded shape-selective monofunctional (metal)[2] and bifunctional (metal,

* To whom correspondence should be addressed.
[†] Department of Chemical Engineering.
[‡] Shell Development Company.

(1) Chen, N. Y.; Garwood, W. E.; Dwyer, F. G. *Shape Selective Catalysis in Industrial Applications*; Marcel Dekker: New York, 1989.
(2) Hughes, T. R.; Buss, W. C.; Tamm, P. W.; Jacobson, R. C. *Stud. Sur. Sci. Catal.* **1986**, *28*, 725.

0022-3654/90/2094-6425$02.50/0

acid site)[3] catalysts. Heteroatom, e.g., Fe, Co, B, substitution for framework aluminum (Al^{3+}) in zeolites has been reported[4] and has been shown to modify the acidity of the zeolite. We were the first to show that cobalt can substitute for framework aluminum in ZSM-5.[5] In that case, cobalt had an oxidation state of 2 and thus modified the acidity from that observed for ZSM-5.[6] After synthesizing cobalt ZSM-5 and elucidating its physicochemical properties, we initiated research to exploit the advantages of having isolated atoms within molecular sieve frameworks that could undergo changes in oxidation state. For example, tetrahedral Co^{2+} is common, and although tetrahedral Co^{3+} is rare, it is known to exist.[7] Thus, the possibility of creating isolated redox centers within a microporous environment appeared high. One particularly appealing application for this type of material would be for use as a shape-selective partial oxidation catalyst.

At the time of completing our cobalt ZSM-5 work, Union Carbide announced metal-substituted aluminophosphate molecular sieves.[8] Elements such as Mg, Mn, Zn, Co, and Ti were claimed to substitute into the aluminophosphate ($AlPO_4$-*n*)[9] lattice to form what was called MeAPO-*n* molecular sieves, e.g., CoAPO-*n* for cobalt substitution. From the elemental compositions listed in the Union Carbide patents, it appeared that higher levels of substitution were possible in the $AlPO_4$'s than with zeolites, i.e., there was more cobalt in CoAPO materials than our cobalt ZSM-5. Also, strong evidence was available to suggest that Co^{2+} substitutes for Al^{3+} in forming CoAPO-5 and CoAPO-11.[10] Thus, we began our study of isolated redox centers in microporous environments with the $AlPO_4$'s rather than zeolites.

The purpose of our work is to synthesize pure phase MeAPO's where Me is an element that can have multiple oxidation states and remain within the oxide framework and to characterize their physicochemical properties as well as their oxidation–reduction chemistry. Our initial efforts involved cobalt- and vanadium-substituted $AlPO_4$-5.[11] This paper reports results from CoAPO-5 while the accompanying paper concentrates on VAPO-5.[12] Since completion of our work, three papers have appeared that concern cobalt aluminophosphates[13-15] and these results will be compared to our data. None of these studies have shown that a variety of cobalt environments exist and that only the framework sites can be oxidized/reduced as we have demonstrated here.

Experimental Section

The X-ray powder diffraction pattern of all samples was recorded and indexed on a Siemens I2 automated diffraction system. The complete powder patterns of samples after calcination in flowing oxygen to 500 °C were indexed by using a magnesium–aluminum spinel as the internal standard.

Thermogravimetric analyses (TGA) and differential thermal analyses (DTA) were performed in air on a Dupont 951 thermogravimetric analyzer and a 1600 °C differential thermal analyzer, respectively, and were used to estimate the organic and water contents.

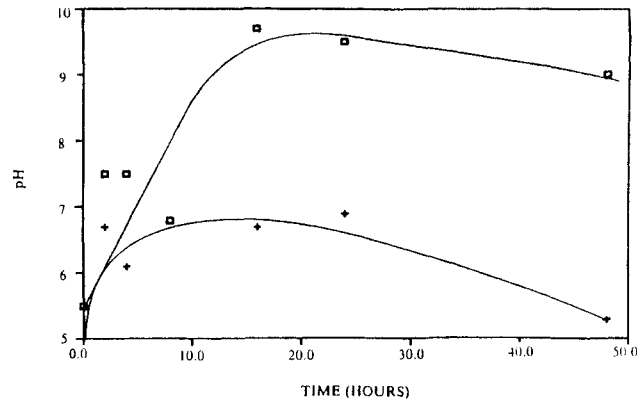

Figure 1. pH profile from synthesis of CoAPO-5 (+) and $AlPO_4$-5 (□).

Argon adsorption isotherms were obtained at liquid argon temperatures on an Omnisorp 100 analyzer. Argon adsorption capacities and X-ray diffraction patterns were used to ascertain phase purity.

Bulk chemical analyses of the solid samples (after dissolution into HCl solutions) and the chemical analysis of ion exchange solutions were performed by using an inductively coupled plasma (ICP) spectrometer. The ICP system consisted of a Jarrell-Ash ICAP 9000 and a Jarrel-Ash Atomscan 2400.

Scanning electron micrographs (SEM's) were recorded on a Cambridge Instruments Steroscan 200 microscope.

Diffuse reflectance electronic absorption spectra from 200 to 700 nm were obtained on neat, powdered samples, using a Shimadzu CS-9000 spectrometer.

Magic angle spinning ^{31}P NMR spectra were recorded on a Bruker CXP 200 spectrometer. The ^{31}P spectra were taken at a frequency of 80.4 MHz and with sample spinning rates of 4–5 kHz. Chemical shifts are reported relative to 85 wt % H_3PO_4. Magic angle spinning ^{27}Al NMR spectra were recorded on a Bruker CXP-200/400 spectrometer. The ^{27}Al spectra were taken at a frequency of 104.3 MHz and a rotation rate of 3–5 kHz. The ^{27}Al chemical shifts are reported relative to $Al(NO_3)_3$ in aqueous solution at infinite dilution and are not corrected for second-order quadrupole effects. Chemical shifts downfield of the standard are expressed as positive shifts.

Electron paramagnetic resonance (ESR) spectra were recorded on an IBM ER 200D spectrometer at a microwave frequency of 9.495 GHz. Spectra were obtained at 77 K and 298 K. The samples were sealed in quartz tubes and referenced to DPPH.

Results and Discussion

CoAPO-5 was synthesized by heating a gel with composition $1.5Et_3N{\cdot}0.8Al_2O_3{\cdot}0.4CoO{\cdot}P_2O_5{\cdot}40H_2O$ to 200 °C at autogenous pressure. The gel was prepared by combining H_3PO_4, pseudoboehmite alumina, triethylamine, and cobalt sulfate with water. $AlPO_4$-5 was synthesized for comparison with CoAPO-5 by heating a gel with composition $1.5Et_3N{\cdot}Al_2O_3{\cdot}P_2O_5{\cdot}40H_2O$ to 200 °C at autogenous pressure. The complete details of these syntheses are available elsewhere.[11] Autoclaves were removed from a 200 °C forced convection oven at specified times and quenched in cold water, and the pH of the contents was measured. Product crystals were recovered by slurrying the autoclave contents in water, stirring for several minutes, allowing the solids to settle, and discarding the supernatant liquid. This procedure was repeated several times until a clear liquid was obtained. Then, the solid was filtered and dried at room temperature. Shiralkar et al.[15] synthesized CoAPO-5 by a procedure similar to that used here but never obtained a pure sample. From the results of all tests available to us (vide infra), we believe that our samples are pure. The difference from Shiralkar et al.[15] may be our recovery and cleaning procedure.

Figure 1 shows the pH of the autoclave contents as a function of heating time for the synthesis of CoAPO-5 and $AlPO_4$-5. For

(3) Engelen, C. W. R.; Wolthuizen, J. P.; van Hooff, J. H. C.; Zandbergen, H. W. *Stud. Sur. Sci. Catal.* **1986**, *28*, 709.
(4) Szostak, R. Molecular Sieves: *Principles of Synthesis and Indentification*; van Nostrand Reinhold: New York, 1989.
(5) Rossin, J. A.; Saldarriaga, C.; Davis, M. E. *Zeolites* **1987**, *7*, 295.
(6) Wolf, E. E., personal communication.
(7) (a) Shimura, Y.; Tsuchida, R. *Bull. Chem. Soc. Jpn.* **1957**, *30*, 502. (b) Wood, D. L.; Remeika, J. P. *J. Phys. Chem.* **1967**, *46*, 3595. (c) Simmons, V. E. Ph.D. Thesis, Boston Univ., Boston, MA, 1963. (d) Cotton, F. A.; Wilkinson, G. *Advanced Inorganic Chemistry*; Wiley: New York, 1980.
(8) (a) Wilson, S. T.; Flanigen, E. M. Eur. Patent Appl. 0132708, 1985. (b) Wilson, S. T.; Flanigen, E. M. U.S. Patent 4,567,029, 1986.
(9) The suffix *n* denotes a specific structure type as given in ref 8.
(10) Tapp, N. J.; Milestone, N. B.; Wright, L. J. *J. Chem. Soc., Chem. Commun.* **1985**, 1801.
(11) Montes, C. Ph.D. Dissertation, Virginia Polytechnic Institute and State University, Blacksburg, VA, May 1989.
(12) Montes, C.; Davis, M. E.; Murray, B.; Narayana, M. *J. Phys. Chem.*, following paper in this issue.
(13) Schoonheydt, R. A.; de Vos, R.; Pelgrims, J.; Leeman, H. *Stud. Sur. Sci. Catal.* **1989**, *49*, 559.
(14) Iton, L. E.; Choi, I.; Desjardins, J. A.; Maroni, V. A. *Zeolites* **1989**, *9*, 535.
(15) Shiralkar, V. P.; Saldarriaga, C. H.; Perez, J. O.; Clearfield, A.; Chen, M.; Anthony, R. G.; Donohue, J. A. *Zeolites* **1989**, *9*, 474.

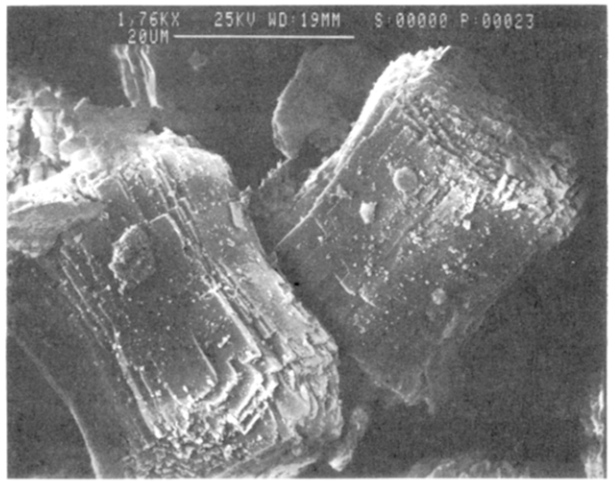

Figure 2. Scanning electron micrograph of CoAPO-5.

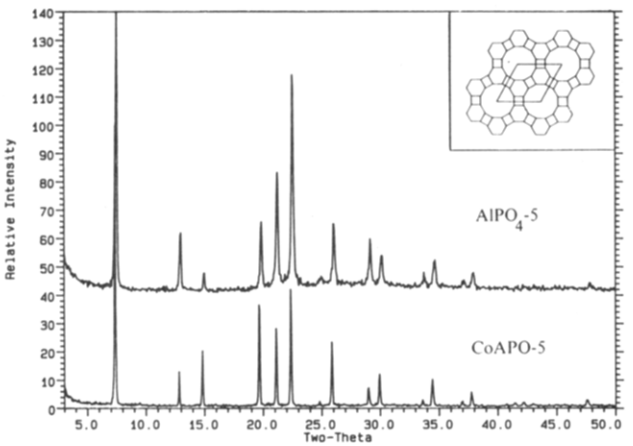

Figure 3. X-ray powder diffraction patterns from $AlPO_4$-5 and CoAPO-5. Inset: framework [001] projection of topology.

$AlPO_4$-5, the pH begins around 5.5 and rises to almost 10 over a period of 20 h. After 2 h of heating, pure $AlPO_4$-5 is obtained. At heating times longer than 16 h, $AlPO_4$-5 begins to lose crystallinity and other crystalline phases appear in the collected solids. It is not surprising that $AlPO_4$-5 loses crystallinity at longer heating times since a phosphate-containing framework is not likely to be stable at such high pH. The pH profile from the CoAPO-5 synthesis is lower than that from $AlPO_4$-5 and is most probably due to H_2SO_4 formed from the cobalt sulfate. Pure CoAPO-5 is obtained in 2–6 h of heating. At longer heating times a second phase, most likely CoAPO-47, appears in addition to CoAPO-5.

Figure 2 shows an SEM of CoAPO-5. The particles appear "barrel-like" and are 40 μm by 20 μm aggregates of the CoAPO-5 crystals. This morphology has been observed also for $AlPO_4$-5[16,17] and for SAPO-5,[17] the silicon-containing analogue of $AlPO_4$-5.

Figure 3 shows the X-ray diffraction patterns of $AlPO_4$-5 and CoAPO-5 and a schematic of the [001] framework projection of their topology. The symmetry of $AlPO_4$-5 is hexagonal and the unit cell contains 24 tetrahedral oxide units: 12 Al and 12 P. The topology consists of unidimensional channels circumscribed by rings containing 12 teterahedral atoms with diameter of 7–8 Å.[18] The X-ray diffraction pattern of $AlPO_4$-5 shown here is in agreement with those published previously.[16-18] Since the X-ray diffraction pattern of CoAPO-5 is nearly the same as that for $AlPO_4$-5, it is clear that CoAPO-5 possesses the same framework topology as $AlPO_4$-5. The bulk chemical composition of $AlPO_4$-5 and CoAPO-5 are $0.24Et_3N{\cdot}Al_2O_3{\cdot}P_2O_5{\cdot}0.36H_2O$ and $0.21Et_3N{\cdot}0.8Al_2O_3{\cdot}P_2O_5{\cdot}0.4CoO{\cdot}0.63H_2O$, respectively. Although the organic molecules are listed as the amine for CoAPO-5, it is most likely that the amine has been protonated (vide infra). Notice that Al/P = 1 for $AlPO_4$-5, as expected. If all of the cobalt were to substitute for aluminum in the CoAPO-5 framework, a significant increase in the size of the unit cell would be expected since Co^{2+} (0.72 Å)[19] is much larger than Al^{3+} (0.52 Å).[19] The measured unit cell dimensions for the $AlPO_4$-5 and CoAPO-5 used here are a = 13.61 Å, c = 8.47 Å, V = 1359 Å^3, and a = 13.70 Å, c = 8.44 Å, V = 1372 Å,^{3} respectively. The unit cell of $AlPO_4$-5 reported here is smaller than that reported previously for calcined $AlPO_4$-5.[20] However, the unit cell dimensions of $AlPO_4$-5 have been observed to vary with the nature of the organic template.[11] Thus, we report here data for $AlPO_4$-5 and CoAPO-5 that have been synthesized with the same template. Although there is an increase in the unit cell size with the addition of cobalt, it is not as large as expected if all the cobalt were sited within the framework. Thus, it appears that only a portion of the cobalt has substituted for aluminum within the framework. Further evidence is provided below to support this premise. Our unit cell calculations cannot be directly compared to those of Shiralkar et al.[15] because they do not report the composition of their solids (they report only the gel composition) and because their samples were not calcined.

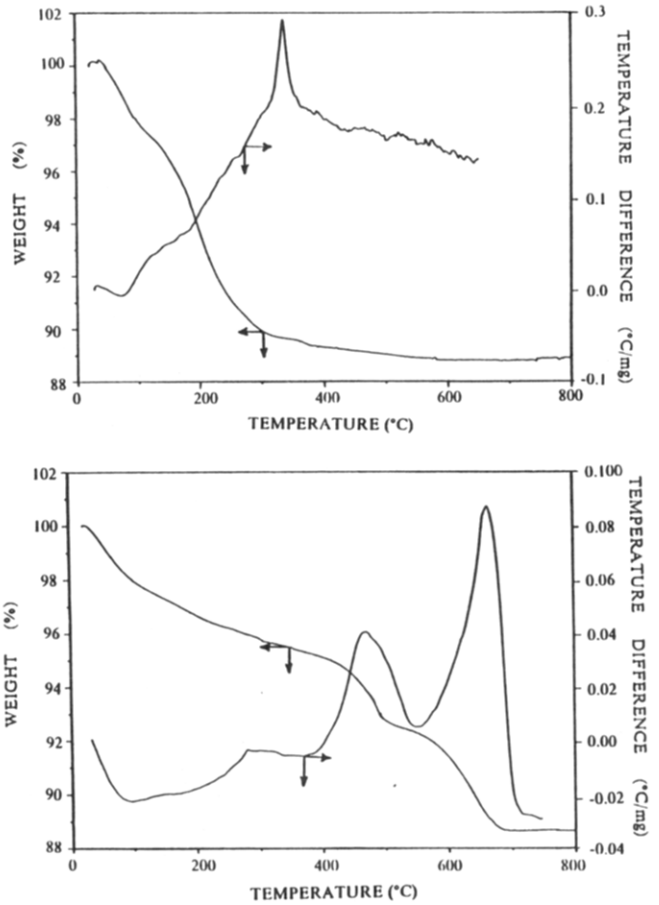

Figure 4. Thermogravimetric and differential thermal analyses from $AlPO_4$-5 (top) and CoAPO-5 (bottom). Heating rate = 20 °C/min.

Figure 4 shows the TGA and the DTA from $AlPO_4$-5 and CoAPO-5. The initial, small endotherm and associated weight loss from $AlPO_4$-5 is due to the desorption of water. The Et_3N is lost over the temperature range of 100–400 °C. From the TGA, approximately 1.41 molecules of Et_3N are present per unit cell of $AlPO_4$-5. This result compares well to that reported elsewhere

(16) Wilson, S. T.; Lok, B. M.; Messina, C. A.; Cannan, T. R.; Flanigen, E. M. *ACS Symp. Ser.* **1983**, *218*, 109.
(17) Van Nordstrand, R. A.; Santilli, D. S.; Zones, S. I. *ACS Symp. Ser.* **1988**, *368*, 236.
(18) Bennett, J. M.; Cohen, J. P.; Flanigen, E. M.; Pluth, J. J.; Smith, J. V. *ACS Symp. Ser.* **1983**, *218*, 109.
(19) Shannon, R. D. *Acta. Crystallogr.* **1976**, *A32*, 751.
(20) Richardson, J. W., Jr.; Pluth, J. J.; Smith, J. V. *Acta Crystallogr., Sec. C* **1987**, *C43*, 1469.

TABLE I: Chemical Composition of Solids and Liquids after Ion Exchange

	solid			filtrate (μmol/mL)		
sample	Na/P	Co/P	Al/P	Co	Al	P
as-synthesized CoAPO-5	0.0133	0.1681	0.8171	0.0051	0.0074	0.016
O_2-calcined CoAPO-5	0.0471	0.1121	0.8630	0.1900	0.0074	0.1453

for $AlPO_4$-5.[16] For CoAPO-5, there is a larger endotherm and associated weight loss than observed with $AlPO_4$-5, indicating a greater water content in CoAPO-5. Also, the exotherm due to the combustion of the organic in CoAPO-5 occurs at higher temperatures and in multiple steps. (Our TGA/DTA data are very similar to those reported by Shiralkar et al.[15]) The organic content is estimated to be 1.27 molecules per unit cell in CoAPO-5, and because of the shape of the TGA/DTA, we believe that at least a portion of the triethylamine is protonated. Since the substitution of Co^{2+} for Al^{3+} will yield a negative charge on the framework,[10,21] the protonated amine can balance the anionic framework charge. Thus, the TGA/DTA patterns indicate that at least some of the cobalt present in CoAPO-5 is sited within the framework.

If only a portion of the cobalt substitutes for framework aluminum, then some of the cobalt will be located within the pores. This extraframework cobalt should be ion exchangeable with other cations. However, since the as-synthesized CoAPO-5 contains the organic molecules within the unidimensional channel system, it was first necessary to calcine CoAPO-5 prior to ion exchange. CoAPO-5 was calcined at 500 °C in flowing, dry O_2 to remove the organic material. This treatment removes all organics. If the sample is heated to 500 °C in air such is not the case (see TGA/DTA). Shiralkar et al.[15] noticed structural collapse of CoAPO-5 upon heating to 550 °C in air. Here no structural loss is observed by X-ray powder diffraction after treatment with flowing, dry O_2 at 500 °C. Table I lists the chemical composition of the solids and filtrates obtained after treating approximately 120 mg of solid with 50 mL of 0.1 N NaCl for 20 h with stirring (starting material has the same Co/P and Al/P as the treated as-synthesized sample). The as-synthesized CoAPO-5 is used as a control to obtain background levels of Na, Co, Al, and P since no exchange is expected when the channels are clogged by the organic. (No adsorption of Ar is observed from this sample, indicating that the organic is still blocking access to the main channels; since Co^{2+} cannot diffuse through six-membered rings it is trapped as well.) The data given in Table I clearly show that some of the cobalt is readily ion-exchanged out of the O_2-calcined CoAPO-5. Notice that the filtrate contains phosphorus as well as cobalt. The phosphorus loss is reflected also in the elemental ratios of the solid, i.e., the Al/P increases after exchange. Thus, CoAPO-5 appears to contain extraframework cobalt and phosphorus. Very recently, occluded phosphorus has been reported and speculated to be in the form $H_2PO_4^-$ and balance charge of an organic (Et_4N^+) in $AlPO_4$-52.[22] For the case of CoAPO-5, anionic charges could be from framework substitution of Co^{2+} for Al^{3+} and from occluded $H_2PO_4^-$ (or HPO_4^{2-}, PO_4^{3-}) and balance positive charges from occluded Et_3NH^+ and Co^{2+}.

If occluded cobalt and phosphorus exist in CoAPO-5, then the space they occupy should be directly observable through adsorption studies. Figure 5 shows the argon adsorption isotherms from calcined $AlPO_4$-5, CoAPO-5, and CoAPO-5 after exchange with 0.1 N NH_4Cl. CoAPO-5 was calcined in oxygen, exchanged with NH_4Cl, and calcined again to remove any extraframework components and leave behind only H^+ as the balancing cations ($NH_4^+ \rightarrow H^+$ upon heated above 350 °C) in order to compare to $AlPO_4$-5. The isotherms are plotted as the relative uptake (WO is the final uptake) against the log of the relative pressure for better illustration of the results. Notice that the transition pressure (P/P_0 where the inflection point in the isotherm will occur) occurs at a lower P/P_0 for CoAPO-5 than for $AlPO_4$-5 and that after exchange the two are coincident. We have shown previously that the transition pressure increases with increasing pore size.[23] Thus, the effective pore diameter of CoAPO-5 is smaller than that of $AlPO_4$-5. Since the effective pore diameter returns to that of $AlPO_4$-5 after CoAPO-5 is exchanged, these isotherms clearly indicate the presence of occluded material within the channels of CoAPO-5.

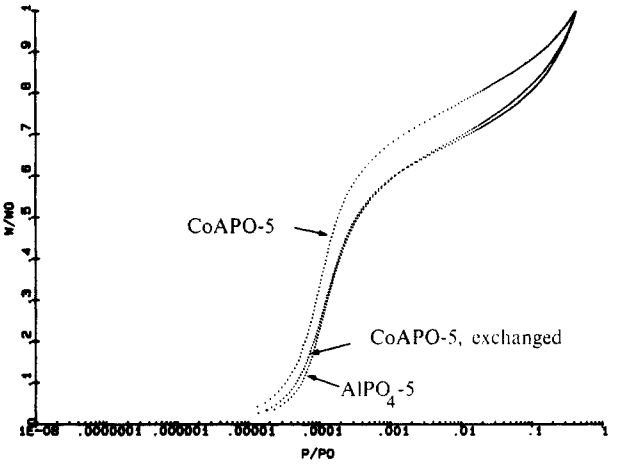

Figure 5. Argon adsorption isotherms.

Figure 6 illustrates the ^{27}Al and ^{31}P MAS NMR spectra from as-synthesized $AlPO_4$-5 and CoAPO-5. For $AlPO_4$-5, single resonances at 37.2 ppm and −29.1 ppm in the ^{27}Al and ^{31}P spectra, respectively compare well to those reported by Blackwell and Patton (after correction for second-order quadrupole effects in the ^{27}Al NMR spectrum).[24] Since $AlPO_4$-5 contains single crystallographic sites for aluminum and phosphorus, one resonance is expected in the ^{27}Al and ^{31}P MAS NMR spectra. Also, the chemical shifts are indicative of tetrahedral oxide environments with phosphorus (for aluminum) and aluminum (for phosphorus) second nearest neighbors.[22] The ^{27}Al and ^{31}P MAS NMR spectra from CoAPO-5 shows also single resonances at 37.5 ppm and −27.9 ppm, respectively. The other peaks are spinning sidebands (confirmed by variations in spinning frequencies). These sidebands arise from strong dipolar interactions with paramagnetic cobalt. The ^{27}Al and ^{31}P MAS NMR spectra of as-synthesized CoAPO-5 and FeAPO-5 (iron-substituted $AlPO_4$-5) exhibit numerous sidebands while $AlPO_4$-5 and MgAPO-5 do not. The static ^{31}P NMR spectrum of CoAPO-5 shows a single broad resonance with a peak at approximately −29 ppm. The small change in the chemical shift suggests that the ^{31}P MAS NMR spectrum is the result of contributions from both dipolar interactions and chemical shift anisotropy. The anisotropy observed in the ^{31}P MAS NMR spectrum supports the view that cobalt is primarily substituting for framework aluminum. If cobalt is substituting for aluminum in the framework, then one would expect more than a single resonance in the ^{31}P spectrum. However, notice that the width of the ^{31}P peak is larger for CoAPO-5 than for $AlPO_4$-5. Thus, for CoAPO-5, the resolution may not be sufficient to observe the presence of two environments within the broad resonance centered around −27.9 ppm. Also, there is a small signal intensity around 0 ppm in the ^{31}P MAS NMR spectrum from CoAPO-5, which may be due to occluded phosphate.

Upon calcination of CoAPO-5 in flowing O_2 at 500 °C, the sample turns yellow-green in color. Also, subsequent contact of the oxidized sample with flowing H_2 at 500 °C returns the color to blue. We have found also that contact of the yellow-green sample with room-temperature vapors of methanol and acetone also return the color to blue. These treatments and color changes

(21) Bennett, J. M.; Marcus, B. K. *Stud. Sur. Sci. Catal.* **1988**, *37*, 269.
(22) Bennett, J. M.; Kirchner, R. M.; Wilson, S. T. *Stud. Sur. Sci. Catal.* **1989**, *49A*, 731.
(23) Davis, M. E.; Montes, C.; Hathaway, P. E.; Arhancet, J. P.; Hasha, D. L.; Garces, J. M. *J. Am. Chem. Soc.* **1989**, *111*, 3919.
(24) Blackwell, C. S.; Patton, R. L. *J. Phys. Chem.* **1984**, *88*, 6135.

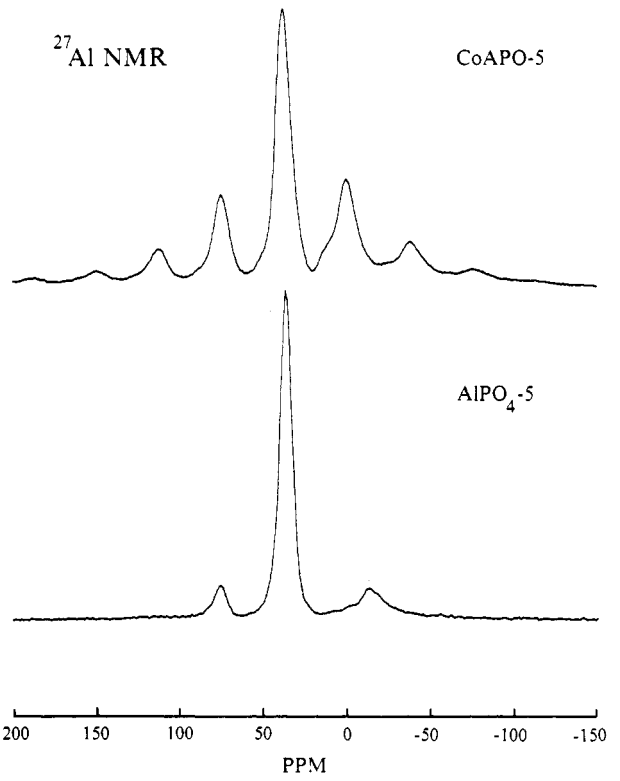

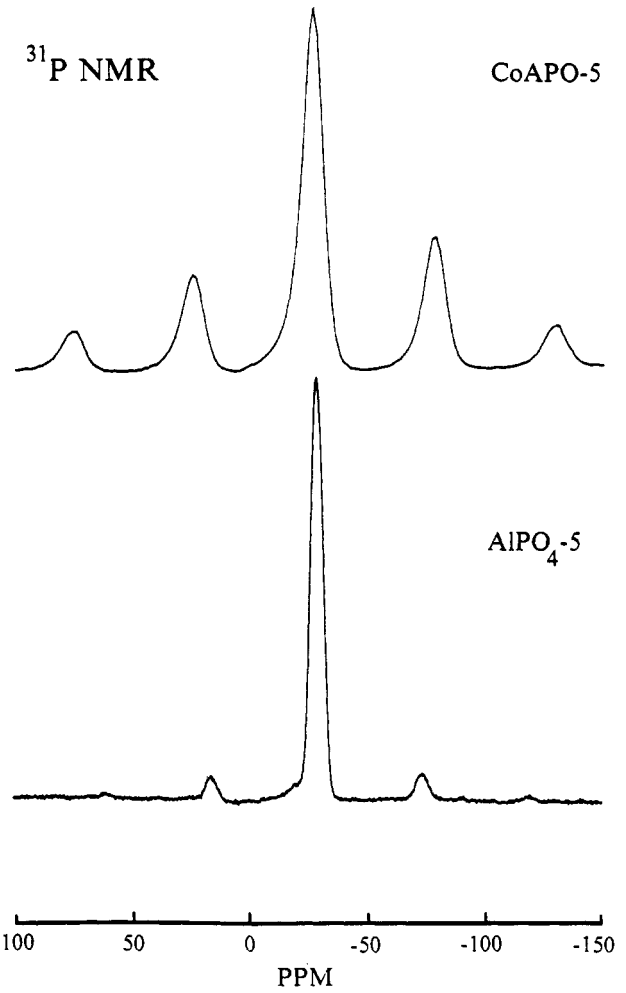

Figure 6. Solid-state NMR spectra from $AlPO_4$-5 and CoAPO-5: ^{27}Al (top); ^{31}P (bottom).

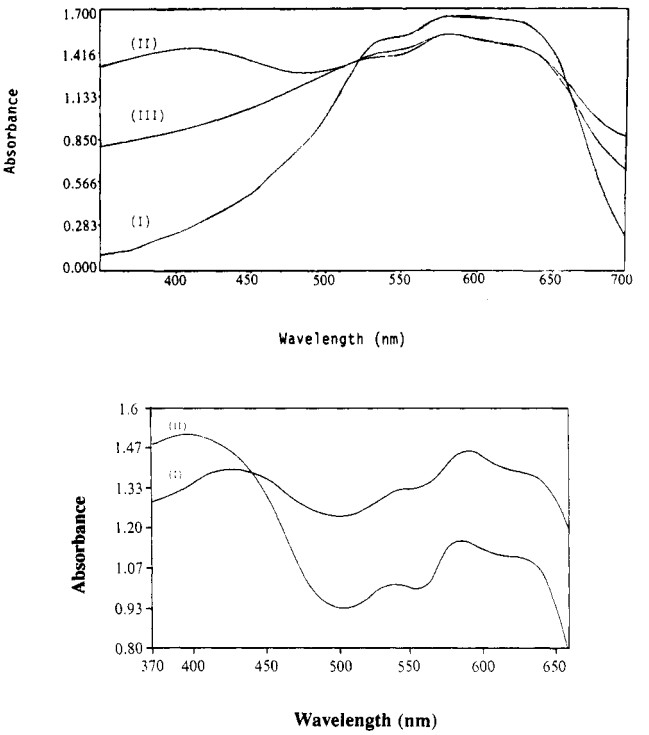

Figure 7. Electron absorption spectra: (top) I, as-synthesized; II, calcined in O_2; III, calcined in O_2 then exposed to H_2; (bottom) I, calcined in O_2; II, calcined in O_2, ion-exchanged with NH_4Cl, then calcined in O_2 again.

led us to believe that Co^{2+} could be oxidized to Co^{3+} and then reduced back to Co^{2+} again. Below we provide spectroscopic evidence to support this premise.

Figure 7 shows the electronic absorption spectra over the energy range of 350–700 nm for CoAPO-5 treated in several ways. The as-synthesized sample shows absorptions in the 500–650-nm region. These absorptions are from the $^4A_2 \rightarrow {}^4T_1(P)$ transitions of high-spin (d^7) Co^{2+} (ref 7) and clearly indicate that some of the cobalt is sited within the CoAPO-5 in tetrahedral coordination. Upon oxidizing CoAPO-5, the absorption intensities in the 500–600-nm region decrease and a new absorption at ~415 nm appears. Contact of the oxidized sample with flowing H_2 at 500 °C begins to remove the band at ~410 nm. We assign the absorption at 410 nm to tetrahedral Co^{3+}. Thus, after treatment with O_2, Co^{2+} and Co^{3+} exist in CoAPO-5. Since cobalt resides within the framework and as extraframework cations, the mixed oxidation states may arise from the different cobalt species. CoAPO-5 was calcined in air to remove the organic template to test this thought. Next, the extraframework cobalt was exchanged for NH_4^+. Finally, the exchanged sample was calcined in flowing O_2 at 500 °C. The absorption spectrum from this sample is shown in Figure 7 also. Notice that the 410 nm absorption is now much more intense than the absorptions at 500–650 nm. Since we could not transfer the O_2-calcined sample into the spectrometer without exposure to ambient air, we believe that the bands at 500–650 nm are due to ambient moisture reducing Co^{3+} to Co^{2+} upon sample transfer. We show below that O_2 treatment does in fact convert all of the Co^{2+} to Co^{3+}.

Schoonheydt et al.[13] very recently reported electronic absorption spectra for CoAPO-5. They observed bands at 625, 578, and 540 nm from as-synthesized CoAPO-5. These absorptions are in excellent agreement with our data. Schoonheydt et al. report also an absorption at 390 nm for CoAPO-5 which has been oxidized. This band is most likely the same as we observe around 410 nm. Thus, our as-synthesized and oxidized spectra compare well to Schoonheydt et al.

Table II lists the ligand field strengths for cobalt in environments that contain all oxygen nearest neighbors. It is clear from these data that both Co^{2+} and Co^{3+} in CoAPO-5 are tetrahedrally coordinated.

TABLE II: Ligand Field Strength, Dq, for Cobalt in Oxygen Environments

sample	cobalt oxidn state	cobalt coordntn	Dq, cm^{-1}	ref
$[CoO_4W_{12}O_{36}]^{-6}$	+2	4	484	7c
$[CoO_4W_{12}O_{36}]^{-5}$	+3	4	800	7c
garnet	+2	4	460	7b
garnet	+2	6	920	7b
garnet	+3	4	830	7b
garnet	+3	6	1600	7b
CoAPO-5	+2	4	380	23 and this work[a]
CoAPO-5	+3	4	900	23 and this work[a]

[a] By comparison of the spectra shown here to those in ref 23.

Iton et al.[14] very recently reported that CoAPO-34 and CoAPSO-34 can contain Co^{3+} after oxidation (O_2 at 500–550 °C). The showed absorption spectra that appear qualitatively similar to those illustrated here. The only proof given by Iton et al.[14] for framework siting of cobalt is that hydroxyl groups are present. No chemical analysis is provided to indicate the level of cobalt substitution and whether multiple cobalt environments are present. Also, Iton et al. did notice that methanol exposure restored Co^{3+} to Co^{2+} and postulated the reaction product to be $H_2C{=}O$. Unfortunately, Iton et al. did not collect the reaction products (neither did we on CoAPO-5).

The picture that emerges so far is that cobalt resides within the framework and as extraframework cations in the 2+ oxidation state. The cobalt that is sited within the framework is capable of being oxidized to Co^{3+} and remains in the lattice. The extraframework cobalt is not oxidized. Thus, the framework stabilizes Co^{3+} in tetrahedral geometry. The Co^{3+} is easily reducible back to Co^{2+}. Therefore, isolated redox centers are in fact produced in CoAPO-5.

In order to test the conjectures given above, we performed ESR experiments on $AlPO_4$-5 and CoAPO-5 at 77 K and 298 K. The $AlPO_4$-5 sample did not display an ESR signal as expected (see Figure 8). The as-synthesized CoAPO-5 ESR spectrum recorded at 77 K is shown in Figure 8. A single resonance is seen with a g value of 2.030 ± 0.002. The spectrum is consistent with Co^{2+} occupying a framework position. However, no hyperfine structure is observed. The lack of hyperfine structure, (^{59}Co, $I = 7/2$), may be due to strong spin–spin interactions between cobalt neighbors. This is expected since the substitution of Co^{2+} for Al^{3+} creates an anionic framework charge that requires a charge compensating species (such as Co^{2+} ions) to reside nearby.

A sample of CoAPO-5 was calcined in flowing O_2 at 500 °C and then ion-exchanged with an 0.1 N NH_4Cl solution. The ion-exchanged sample was again calcined in flowing O_2 at 500 °C and transferred to the ESR sample tube under an inert atmosphere in a glovebox. No ESR signal is apparent from this material at 298 K, but a very broad signal is witnessed at 77 K (see Figure 8). The signal observed for as-synthesized CoAPO-5 is not seen. These spectra support the view that cobalt has been oxidized. The ^{31}P MAS NMR spectrum of this sample is essentially identical with that of the as-synthesized CoAPO-5 (shown in Figure 6B), indicating that an interaction with paramagnetic cobalt is still giving rise to the numerous sidebands in the spectrum. The fact that the ^{31}P MAS NMR spectrum is essentially unchanged may suggest that the ESR spectrum of the treated sample probably needs to be recorded at a lower temperature in order to obtain useful structural details.

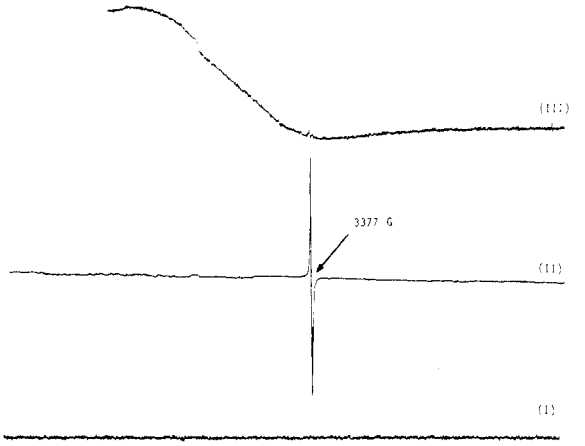

Figure 8. Electron spin resonance spectra: I, $AlPO_4$-5; II, as-synthesized CoAPO-5; III, CoAPO-5 calcined in O_2 ion-exchanged with NH_4Cl, then calcined in O_2 again.

Finally, several other techniques were explored to further investigate these materials. X-ray photoelectron spectroscopy (XPS) did not show a change in binding energy (within experimental error) from the oxidized and reduced samples. The relatively broad peak width and low surface concentration lead to low signal-to-noise and rendered precise binding energy determinations difficult. EXAFS spectra of the oxidized and reduced samples both reveal pre-edge features indicative of cobalt in tetrahedral coordination. Complete interpretation of the EXAFS data will require further data collections that we expect to perform at a later date.

Acknowledgment. C.M. and M.E.D. acknowledge the financial support of this work by the National Science Foundation and the Dow Chemical Company through the Presidential Young Investigator award to M.E.D.